Development 138, 2511-2521 (2011) doi:10.1242/dev.062505

RanBPM is essential for mouse spermatogenesis and oogenesis

Sandrine Puverel[1], Colleen Barrick[1], Susanna Dolci[2], Vincenzo Coppola[1,3] and Lino Tessarollo[1,*]

SUMMARY

RanBPM is a recently identified scaffold protein that links and modulates interactions between cell surface receptors and their intracellular signaling pathways. RanBPM has been shown to interact with a variety of functionally unrelated proteins; however, its function remains unclear. Here, we show that RanBPM is essential for normal gonad development as both male and female *RanBPM*$^{-/-}$ mice are sterile. In the mutant testis there was a marked decrease in spermatogonia proliferation during postnatal development. Strikingly, the first wave of spermatogenesis was totally compromised, as seminiferous tubules of homozygous mutant animals were devoid of post-meiotic germ cells. We determined that spermatogenesis was arrested around the late pachytene-diplotene stages of prophase I; surprisingly, without any obvious defect in chromosome synapsis. Interestingly, RanBPM deletion led to a remarkably quick disappearance of all germ cell types at around one month of age, suggesting that spermatogonia stem cells are also affected by the mutation. Moreover, in chimeric mice generated with *RanBPM*$^{-/-}$ embryonic stem cells all mutant germ cells disappeared by 3 weeks of age suggesting that RanBPM is acting in a cell-autonomous way in germ cells. *RanBPM* homozygous mutant females displayed a premature ovarian failure due to a depletion of the germ cell pool at the end of prophase I, as in males. Taken together, our results highlight a crucial role for RanBPM in mammalian gametogenesis in both genders.

KEY WORDS: Spermatogenesis, Oogenesis, Germ cell, Meiosis, Scaffold protein, Sterility, Prophase I, Mouse

INTRODUCTION

Scaffolding proteins are important modulators of a variety of physiological functions. They can act as accessories to multiprotein complexes, facilitate interactions with the cell cytoskeleton and modulate signaling of receptors, depending on the protein-interacting domains included in their structure. RanBPM (also known as Ranbp9) is a scaffolding protein belonging to the family of the Ran-binding proteins (RanBPs). Although proteins of this family were originally identified as binding partners of the small Ras-like GTPase Ran, RanBPM does not contain the consensus Ran-binding domain (Beddow et al., 1995). RanBPM is a multimodular protein containing a consensus SPRY domain, which is a protein-protein interaction domain that was initially discovered in the SplA kinase and the ryanodine receptor (Ponting et al., 1997); a LisH (lissencephaly type-1-like homology) motif that is involved in protein dimerization (Gerlitz et al., 2005; Kim et al., 2004); a CTLH domain (C-terminal to LisH) of unknown function that is often found adjacent to the LisH domain; and a CRA motif that is involved in protein interaction (Menon et al., 2004). The LisH-CTLH domain is present in proteins involved in microtubule dynamics, cell migration, nucleokinesis and chromosome segregation and has been recently described in several proteins associated with RanBPM (Emes and Ponting, 2001; Kobayashi et al., 2007). Thus, it is not surprising that RanBPM has been found as a component of a large protein complex of more than 670 kDa (Kobayashi et al., 2007; Nishitani et al., 2001).

Since 2002, RanBPM has been shown to interact with more than 45 different proteins. For example, it interacts with the Met tyrosine kinase receptor facilitating activation of the Ras-Erk pathway (Wang et al., 2002). It binds the kelch-repeat protein muskelin affecting cell morphology (Valiyaveettil et al., 2008). In the immune system, it interacts with the β2-integrin LFA1 (lymphocyte function-associated antigen 1) (Denti et al., 2004), whereas in the nervous system it modulates axonal and neurite outgrowth by affecting the plexin-A receptors, the neural cell adhesion molecule L1 signaling and the neurotrophin receptor TrkB (Cheng et al., 2005; Murrin and Talbot, 2007; Togashi et al., 2006; Yin et al., 2010). In the embryonic neocortex, RanBPM is associated with the citron kinase (CITK), possibly affecting mitosis rate during production of pyramidal neurons (Chang et al., 2010). RanBPM has been involved in disease also. For example, it has been shown to regulate the processing of the amyloid precursor protein APP and amyloid β generation by interacting with the lipoprotein receptor-related protein Lrp, App itself and Bace1, components of pathways that are affected in Alzheimer's disease (Lakshmana et al., 2009). In addition, RanBPM possibly modulates the RNA binding properties of the fragile X mental retardation protein (Menon et al., 2004).

Despite the number of interacting molecules identified so far, the biological significance of these interactions with RanBPM is still unknown. By gene targeting in mouse we investigated the biological function of RanBPM in mammals. Mice lacking RanBPM developed to term and reached adulthood, although some died perinatally. Surviving animals showed a severe atrophy of the gonads. Interestingly, in males, testes developed normally up to one week of age. However, afterwards, seminiferous tubules started to show a

[1]Neural Development Section, Mouse Cancer Genetics Program, Center for Cancer Research, NCI, Frederick, MD 21702, USA. [2]Department of Public Health and Cell Biology, University of Rome Torvergata, 00133 Rome, Italy. [3]Department of Molecular Immunology, Virology and Medical Genetics, Ohio State University, Columbus, OH 43210, USA.

*Author for correspondence (tessarol@mail.nih.gov)

Accepted 28 March 2011

spermatogenesis defect progressively leading to testicular atrophy. The first wave of spermatogenesis was marked by large apoptosis of germ cells, strongly suggesting that spermatocytes are eliminated at the late pachytene-diplotene stages of prophase I. Moreover, RanBPM might affect the maintenance of spermatogonia stem cells. Interestingly, fertility in knockout females was also compromised owing to a germ cell loss before reaching the dictyate arrest. Taken together, our data show that mammalian RanBPM plays a crucial role in both spermatogenesis and oogenesis.

MATERIALS AND METHODS

Generation of *RanBPM*$^{-/-}$ mice

RanBPM$^{-/-}$ mice were generated from a gene-trap RanBPM embryonic stem cell line (Baygenomics database, cell line ID: RHA056). By RT-PCR, we confirmed that the βGeo-containing gene-trap cassette was inserted in the intron following the first RanBPM coding exon. Mutant embryonic stem (ES) cells were injected into C57BL/6^{CR} blastocysts by standard methods to generate chimeric mice that transmitted the mutated allele to their offspring (Reid and Tessarollo, 2009). *RanBPM*$^{+/-}$ mice were backcrossed to the C57BL/6^{CR} background for at least six generations before intercrossing to verify that the observed phenotype was not affected by variations in the genetic background. Mice group-housed under standard conditions with food and water available ad libitum were maintained on a 12 hour light/dark cycle and fed a standard chow diet containing 6% crude fat. All experiments were performed in compliance with the National Institutes of Health guidelines for animal care and use of experimental animals.

RanBPM$^{-/-}$ ES cells were generated by growing *RanBPM*$^{+/-}$ cells in 2 mg/ml G418. Three out of the six clones that had lost the second allele of *RanBPM* were used to generate chimeras.

Immunoprecipitation and western blot analysis of brain and testis lysates

Brains and testes from wild-type (WT) and *RanBPM*$^{-/-}$ mice were homogenized in RIPA lysis buffer (50 mM Tris HCl pH 7.5, 150 mM NaCl, 2 mM EDTA, 1% Triton X-100, 1% sodium deoxycholate, 0.1% SDS, protease inhibitors). Immunoprecipitation of RanBPM from brain lysates was performed overnight at 4°C using a goat anti-RanBPM antibody (AbCam) or an isotype goat serum for negative controls. Proteins were separated by SDS-PAGE, transferred to a PVDF membrane and blotted with a rabbit anti-RanBPM antibody (1:2000, AbCam). Inputs were blotted with an HRP-conjugated anti-β-actin antibody (1:5000, AbCam) to control for loading.

Histological analysis and immunohistochemistry

Mice were euthanized by CO_2 asphyxiation. Testes and ovaries were collected and fixed overnight in 10% formalin and processed for standard Hematoxylin and Eosin staining (H&E). For BrdU labeling, mice received an intraperitoneal injection of 5-bromo-2′-deoxyuridine (BrdU; 150 mg per kg body weight) and were sacrificed 2 hours later. For TUNEL analysis (terminal deoxynucleotidyl transferase-mediated deoxyuridine nick end labeling), sections were stained using the ApopTag kit (Millipore) according to the manufacturer's instructions and counterstained with Eosin. Proliferating cell nuclear antigen (PCNA) labeling was performed using a DAKO ARK Kit, with the PCNA antibody (DAKO) used at 1:50 for 1 hour. Sections were counterstained with Gill's Hematoxylin. Primary antibodies were rabbit anti-MVH (AbCam, 1:500), mouse anti-γH2AX (Millipore, 1:500), rabbit anti-RanBPM (AbCam, 1:200) and rat anti-BrdU (Abd Serotec, 1:400). Secondary antibodies were goat anti-rabbit Alexa Fluor 546 (Invitrogen, 1:1000) and goat anti-mouse Alexa Fluor 488 (Invitrogen, 1:1000). For RanBPM and BrdU immunolabeling, the signal was amplified using biotinylated goat anti-rabbit (Vector, 1:200) or biotinylated goat anti-rat (Vector, 1;200) and either streptavidin Texas Red (Vector, 1:400) or the VectaStain ABC kit (Vector) following the manufacturer's recommendations. Slides were examined using an Axioplan 2 or an Axio Imager Z1 microscope (Zeiss) and pictures were taken using AxioCam HRc and AxioCam MRm cameras (Zeiss) controlled by the Axiovision software.

β-Galactosidase staining

Testes and ovaries were collected, quickly washed with PBS and cryoprotected overnight in PBS containing 30% sucrose. Tissues were then embedded in 7.5% gelatin, 10% sucrose in PBS, frozen and stored at –80°C. Cryostat sections (16 μm) were mounted on Superfrost Plus slides (Fisher Scientific) and stained by incubation for several hours to overnight at 32°C in a 4 mg/ml X-Gal (Sigma), 5 mM potassium ferrocyanide, 5 mM potassium ferricyanide, 2 mM $MgCl_2$ and 0.25% Triton X-100 solution in PBS. Slides were then counterstained with Neutral Red.

RT-PCR

Total RNA was extracted from 3-week-old WT and *RanBPM*$^{-/-}$ mice testes using an RNeasy mini kit (Qiagen) and treated with DNase I (Roche). First-strand cDNA was generated by reverse transcription of 500 ng of RNA using the Superscript III first-strand synthesis system (Invitrogen) and random hexamer oligonucleotides. PCR [1 minute at 94°C, 1 minute at 58°C and 1 minute at 72°C (22 cycles) followed by a 5 minute elongation at 72°C] was performed using a PCR Master Mix (Promega). The primers used were described previously (Tanaka et al., 2000) except for *Hsp70.2* (F: AGTCATCACTGTTCCTGCCTA; R: TAGAGCGAGTCGATCTC-TATG) and β-*actin* (F: GATGGTGGGAATGGGTCAGAA; R: TGGCGTGAGGGAGAGCATAGC). GAPDH and β-actin were used as controls.

Spermatocyte spread preparation and immunofluorescence

Surface spreads of spermatocytes was prepared as described previously (Peters et al., 1997). Briefly, cells were spread in a hypotonic solution directly on the slide and stained for immunofluorescence with rabbit anti-SCP3 (AbCam, 1:500) and anti- γH2AX (Millipore, 1:500) antibodies. Secondary antibodies were goat anti-rabbit Alexa Fluor 546 (Invitrogen, 1:1000) and goat anti-mouse Alexa Fluor 488 (Invitrogen, 1:1000). Images were acquired with an Axioplan 2 microscope (Carl Zeiss Microimaging) and a CCD camera (Photometrics NU200) and processed using SmartCapture 2 software (Digital Scientific, UK). The number of diplotene spermatocytes was expressed as a percentage of the total number of spermatocytes.

Superovulation

Three-week-old female mice were injected intraperitoneally with 0.1 ml of Pregnant Mare Serum Gonadotropin (PMSG; 5IU; Sigma Aldrich). Mice were killed 45 hours later and ovaries were collected for histological analysis.

RESULTS

RanBPM$^{-/-}$ mice exhibit partial neonatal lethality and postnatal growth retardation

To investigate the in vivo biological function of *RanBPM*, we generated mice from embryonic stem cells targeted by gene trap in the first intron of the *RanBPM* gene. The gene trap vector generates a fusion transcript comprising the first ATG containing exon and the βGeo cassette encoding a fusion gene between the β-galactosidase (β-gal) and the neomycin resistance gene (Fig. 1A,B). To determine the effectiveness of the gene trap, brains, which express RanBPM at high levels, were lysed and lysates were immunoprecipitated and analyzed by western blot using an anti-RanBPM antibody. As shown in Fig. 1C, RanBPM was detected in WT but not *RanBPM*$^{-/-}$ brain lysates, confirming that the targeting effectively prevented the production of the RanBPM protein.

RanBPM homozygous mutant mice were viable, yet only ~10%, rather than the expected 25% mutant mice, were obtained from intercrosses of heterozygous mice at weaning age. At embryonic day (E)17.5, *RanBPM*$^{-/-}$ mice were present at the expected frequency, suggesting that the missing mutant mice died postnatally. Indeed, we found that most homozygous mutant mice died immediately after birth for reasons that are still unknown. *RanBPM*$^{-/-}$ mice that survived after birth had a normal life span, although they were significantly smaller than their normal

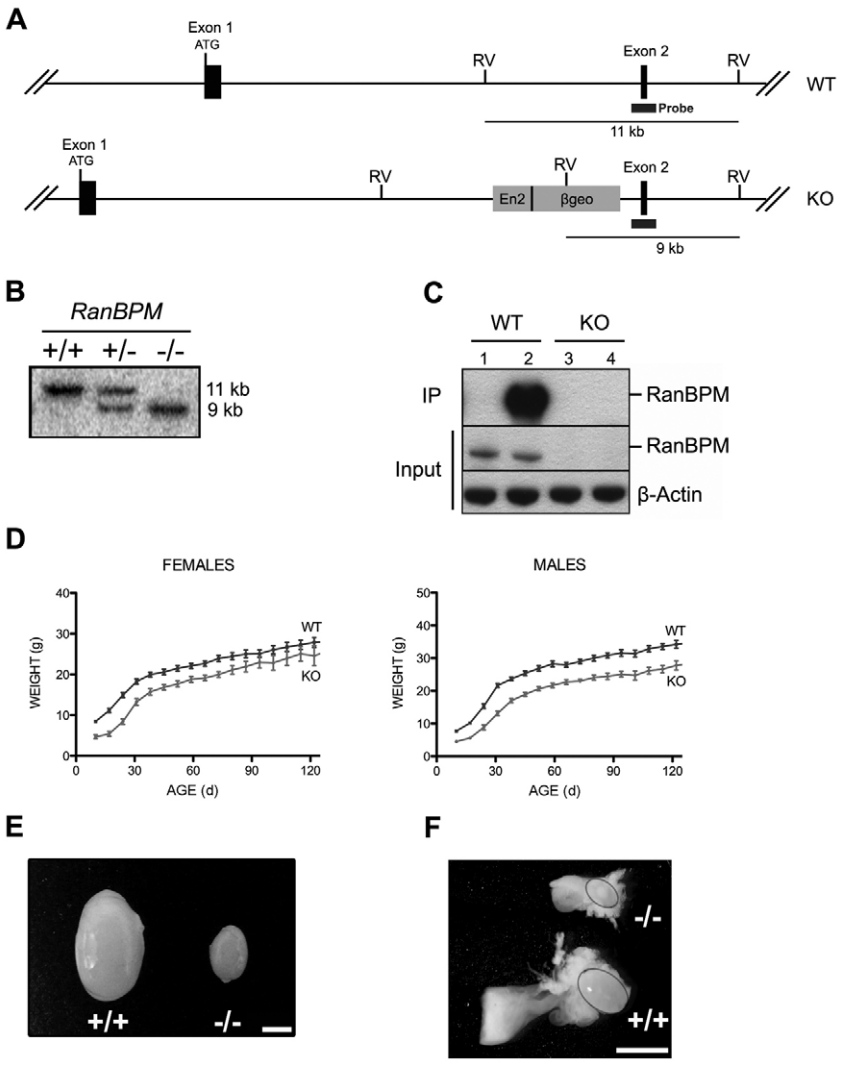

Fig. 1. Targeting of *RanBPM* in mouse causes growth retardation and gonad size reduction. (**A**) Schematic of the *RanBPM* gene targeting. The gene-trap cassette composed of the Engrailed 2 (En2) splice-acceptor sequence and the fusion β-galactosidase-neomycin gene (βGeo) is inserted between exons 1 and 2 causing a change in the size of the *Eco*RV (RV) DNA restriction fragment. (**B**) Southern blot using the probe shown in A and genomic *Eco*RV-digested DNA from wild-type (+/+), heterozygous (+/–) and homozygous (–/–) *RanBPM* mutant mice. (**C**) Western blot analysis of RanBPM protein in lysates from a wild-type (WT) and a knockout (KO) mouse brain. Immunoprecipitation experiments (IP, top panel) show the presence of RanBPM only in the lysates from the WT brain. Protein input is shown in the middle (RanBPM) and bottom (β-actin) panels. Lanes 1 and 3 are negative control IP performed with a goat serum isotype. (**D**) Growth curves for WT and *RanBPM*$^{-/-}$ females (left panel) and males (right panel) over a period of 4 months ($n \geq 12$). (**E**) Representative testes from 1-month-old WT and mutant mice. (**F**) Representative ovaries from 2-month-old WT and mutant mice. Scale bars: 2mm.

littermates (Fig. 1D). The sizes of the main *RanBPM*$^{-/-}$ organs, including brain, heart, liver, lung, kidney, thymus, spleen and intestine were normal relative to the body size and showed no obvious histological defect (data not shown). By contrast, testes and ovaries were strikingly smaller compared with those of WT littermates, and mice of both genders were sterile (Fig. 1E,F).

Spermatogenesis is severely compromised in *RanBPM*$^{-/-}$ males

To investigate the cause of the sterility, we first performed an histological examination of 6-week-old *RanBPM*$^{-/-}$ mouse testes. Contrary to same stage control testes, in which seminiferous tubules were filled with germ cells produced by the spermatogenesis process, seminiferous tubules of *RanBPM*$^{-/-}$ mice were very small and almost completely devoid of germ cells (Fig. 2A,B). The few germ cells still present at this stage were undergoing apoptosis (data not shown). The epididymal duct lumen also lacked sperm (Fig. 2C,D). In older males, we observed that seminiferous tubules were completely empty and undergoing degeneration (Fig. 2E,F). Taken together, these data show that the spermatogenesis process is severely impaired in *RanBPM*$^{-/-}$ male mice, highlighting the essential role of RanBPM for normal male reproductive function. Interestingly, hormone levels in adult male mice, including follicle-stimulating hormone (FSH), luteinizing hormone (LH) and testosterone were comparable to those of control littermates, suggesting an intrinsic role for RanBPM in testis development (data not shown).

Spermatogonia proliferation is reduced in *RanBPM*$^{-/-}$ mice

To investigate at which stage testicular function starts to be affected by the mutation, we examined mutant testes at different time points of postnatal development. At postnatal day (P)0, no difference in testis size was observed between WT and *RanBPM*$^{-/-}$ mice (not shown) and H&E staining revealed normal-sized tubules (Fig. 3A,B). Moreover, using PCNA staining, a marker of proliferation that labels cells in late G1 and S-phase of the cell cycle, we observed proliferating Sertoli cells in both *RanBPM*$^{-/-}$ and control mice (Fig. 3C,D). Gonocytes were also present in *RanBPM*$^{-/-}$ seminiferous tubules, suggesting that the migration of primordial germ cells (PGC) occurred normally (Fig. 3D, arrows). No significant cell death was detected by TUNEL at this stage, either in the WT or in the mutant (data not shown). Similar results were observed at P5: testis size and histology still appeared normal in mutants and germ cell death was absent (Fig. 3E-H). These results suggest that gonocytes migrate normally to the basement membrane of the seminiferous tubules to become undifferentiated type A spermatogonia, the spermatogonial stem cells (SCC).

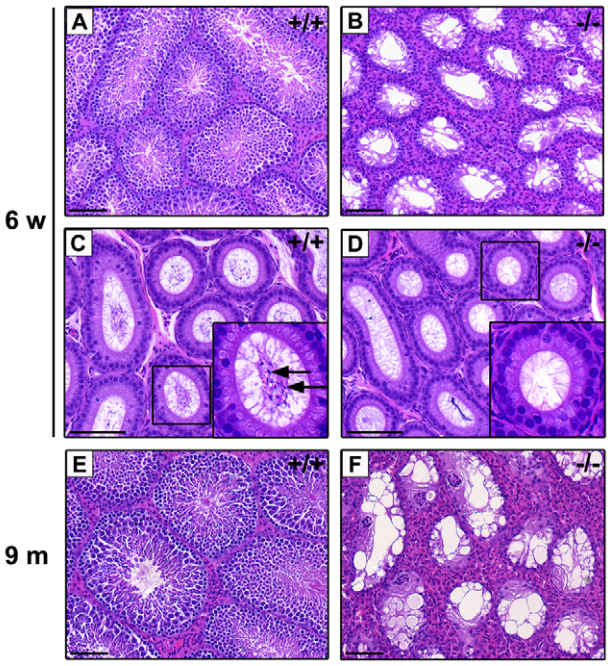

Fig. 2. Sterility of *RanBPM*$^{-/-}$ males. (**A-D**) Hematoxylin and Eosin (H&E)-stained sections of testis (A,B) and epididymis (C,D) from wild-type (+/+; A,C) and knockout (–/–; B,D) 6-week-old (6 w) mice. Mutant seminiferous tubules are almost totally devoid of germ cells (B) and spermatozoa are absent in the mutant epididymis (D). Insets show enlarged views of the boxed areas in C and D. Spermatozoa are indicated by arrows. (**E**,**F**) At 9 months (9 m) mutant tubules (F) are completely degenerated compared with wild type (E). Scale bars: 100 μm.

The second week of male mouse postnatal development is marked by an important proliferation of germ cells along with an increase in testis volume. At this time, we started to see a difference in testis size between *RanBPM*$^{-/-}$ and WT mice coupled to a significant difference in seminiferous tubules size (Fig. 3I,J; data not shown). *RanBPM*$^{-/-}$ tubules were smaller than WT and, although spermatocytes entering meiosis were visible in control testicular sections, they were less numerous on sections from the mutant. Moreover, in *RanBPM*$^{-/-}$ seminiferous tubules, germ cell layers seemed to be less organized and the number of spermatogonia, as well as spermatocytes, appeared to be decreased as revealed by PCNA staining (Fig. 3K,L).

To investigate whether there was a difference in germ cell proliferation, we checked the proliferative status of spermatogonia by in vivo incorporation of BrdU at P8. We found that, contrary to WT testis, where tubules are often delineated by a continuous ring of proliferating spermatogonia, mutant tubules had only sparse and significantly reduced BrdU labeling (Fig. 3M-O). Taken together, these data suggest that the lack of RanBPM affects the proliferation of germ cells after the first week, a time of active mitotic production of spermatogonia.

The first wave of spermatogenesis is abrogated at early meiosis I in *RanBPM*$^{-/-}$ mice

Histological analysis of pubertal (3-week-old) *RanBPM*$^{-/-}$ mouse testis showed that spermatogonia and spermatocytes were present, but post-meiotic cells, i.e. spermatids, were absent, suggesting that the first wave of germ line differentiation did not take place (Fig. 4A-B′). To investigate whether this defect was caused by apoptosis of the germinal cell lineage, we carried out a TUNEL assay. As shown in Fig. 4C-D′, a large number of cells were labeled in the mutant testis, whereas only a few apoptotic cells were detected in the WT testis. These results indicate that, instead of progressing through meiosis, mutant spermatocytes undergo apoptosis and are subsequently eliminated from the seminiferous tubules. To determine more precisely at which meiotic stage the cell differentiation process is disrupted, we performed an RT-PCR expression analysis for stage-specific markers of spermatogenic germ cells at 3 weeks of age, when apoptosis in the mutant was first detected. Genes that display the earliest expression such as *A-myb* (*Mybl1* – Mouse Genome Informatics), which is expressed in spermatogonia and spermatocytes to the pachytene stage (Mettus et al., 1994), *Dmc1*, expressed in leptotene to zygotene spermatocytes (Yoshida et al., 1998) and *Hsp70.2* (*Hspa2* – Mouse Genome Informatics), expression of which is abundant in primary spermatocytes and subsequently decreases in the post-meiotic stages (Rosario et al., 1992; Zakeri et al., 1988), were expressed normally in *RanBPM*$^{-/-}$ mice (Fig. 4E). The *Scp1* (*Sycp1* – Mouse Genome Informatics) and *Scp3* (*Sycp3* – Mouse Genome Informatics) genes, encoding synaptonemal complex proteins (Klink et al., 1997; Meuwissen et al., 1992), were also expressed at normal levels, demonstrating the presence of pachytene spermatocytes in mutant mice. However, the expression of calmegin (Watanabe et al., 1994) and Hox1.4 (Hoxa4 – Mouse Genome Informatics) (Rubin et al., 1986), which starts at the pachytene and persists through the spermatid stage, was significantly reduced in *RanBPM*$^{-/-}$ mice. Moreover, cyclin A1, the level of which has been reported to be upregulated in late pachytene spermatocytes and to peak in diplotene cells, was dramatically reduced (Sweeney et al., 1996). Taken together, these data suggest that in *RanBPM*$^{-/-}$ mice, spermatogenesis is arrested around the late pachytene/diplotene stages of meiotic prophase I.

These observations prompted us to investigate in more details the progression of spermatocytes through meiotic prophase I. Prophase of the first meiotic division involves the pairing, synapsis, recombination and disjunction of homologous chromosomes following tightly regulated mechanisms. Analysis of the synaptonemal complex (SC), a tripartite protein structure that connects paired chromosomes along their entire length (Page and Hawley, 2004), by immunodetection of synaptonemal complex protein 3 (Scp3), a structural component of the axial and lateral elements of the SC (Yuan et al., 2000) showed no difference between the staining pattern of WT and *RanBPM*$^{-/-}$ pachytene and diplotene spermatocytes (Fig. 4F). However, although the formation of the SC appeared to occur normally in mutant cells, the number of diplotene spermatocytes was 60-90% lower than controls (n=3 for each genotype), in accordance with the RT-PCR results. The distribution of phosphorylated histone γH2AX (H2afx – Mouse Genome Informatics), that marks sites of double stranded breaks at the leptotene stage and subsequently converges around the sex chromosomes to form the sex body (Mahadevaiah et al., 2001), also appeared normal in mutant spermatocytes (Fig. 4F), suggesting that synapsis occurs normally in *RanBPM*$^{-/-}$ mice during the first wave of spermatogenesis.

RanBPM is widely and dynamically expressed in the testis

Our data suggest a crucial role for RanBPM in the initiation and maintenance of spermatogenesis. To understand better the function of RanBPM in the testis, we investigated its temporal and spatial pattern of expression by using the *lacZ* reporter gene. At E13.5

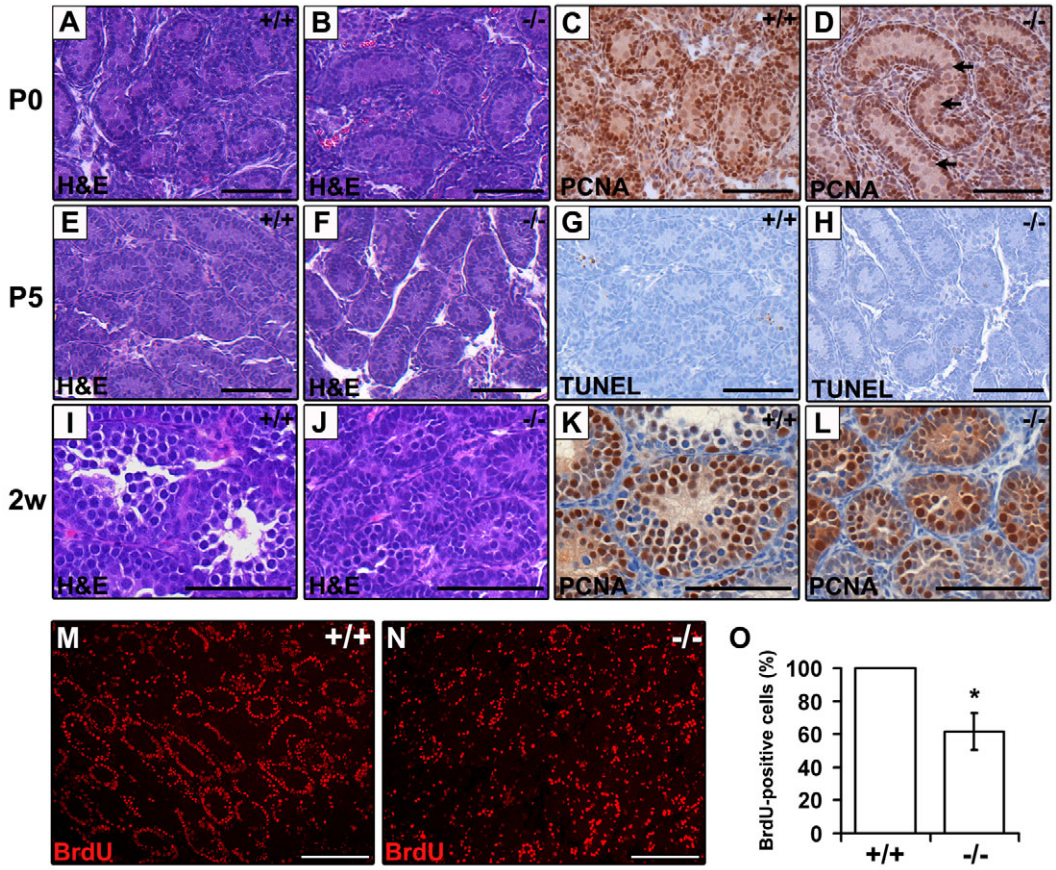

Fig. 3. Reduced spermatogonia proliferation during postnatal testis development. (**A-L**) Paraffin testis sections from postnatal day (P)0 (A-D), P5 (E-H) and 2-week-old (2w; I-L) wild-type (WT; +/+) and mutant (–/–) *RanBPM* mice stained with Hematoxylin and Eosin (H&E) for histology (A,B,E,F,I,J), the proliferation marker proliferating cell nuclear antigen (PCNA) (C,D,K,L) or TUNEL for apoptosis (G,H). At P0, the mutant testis appears normal as, like in WT, Sertoli cells are proliferating (D) and gonocytes (arrows in D) are present. At 2 weeks, mutant tubules are smaller and spermatogonia and spermatocytes are less abundant than in WT. Scale bars: 100 μm. (**M**,**N**) BrdU labeling showing scattered proliferating germ cells (red) in a mutant testis at P8, compared with the even labeling in P8 WT tubules. (**O**) Quantification of BrdU-labeled spermatogonia at P8. Scale bars: 200 μm. Data were obtained from cell number quantification of ten separate fields from each genotype. **P*<0.001, Student's *t*-test.

days of development, we did not find any *RanBPM* expression (data not shown). However, at E17.5, after completion of the gonocyte migration to the gonad, *RanBPM* was expressed in germ cells, as shown by colocalization with the MVH protein (mouse VASA homolog; Fig. 5A,B). At birth, *RanBPM* expression was mainly restricted to the gonocytes (Fig. 5C) whereas five days later it started to be expressed also by the interstitial cells (Fig. 5D). At 2 weeks, expression was detected in both spermatogonia and Sertoli cells (Fig. 5E). In adult mice, we observed a distinct pattern of expression depending on the stage of the seminiferous tubules, suggesting that *RanBPM* expression is dynamically regulated during the spermatogenic wave (Fig. 5F,G). In some tubules, it was detected in spermatogonia residing at the periphery of the tubules (Fig. 5F′). Expression was increased and maintained in both primary and secondary spermatocytes and stopped at the stage of differentiated tailed spermatids that appeared to be devoid of β-gal staining. In other tubule stages, *RanBPM* expression was highly increased in primary spermatocytes (Fig. 5F″). These results are in accordance with other studies that described the expression of RanBPM in cells ranging from spermatocytes to spermatids (Rossi et al., 2004). Interestingly, *RanBPM* expression was increased in spermatocytes undergoing meiosis. Outside the germ cell lineage, RanBPM RNA was highly expressed in Sertoli cells, the supporting cells of the spermatogenic process, and in the interstitial endocrine Leydig cells lying between the seminiferous tubules (Fig. 5F′). Taken together, these data show that *RanBPM* is widely expressed in the adult testis, and its expression seems to be cyclically regulated together with the waves of spermatogenesis.

Expression of RanBPM protein during postnatal development was confirmed by western blot (Fig. 5H). RanBPM protein is expressed at low levels between P1 and 2 weeks but is significantly increased during the third week and later in mature animals, in accordance with the β-gal staining data. Interestingly, immunohistochemistry analysis showed that RanBPM is particularly highly expressed in primary spermatocytes, in accordance with the *lacZ* expression (Fig. 5I,J). Taken together, these data show that RanBPM upregulation coincides with the beginning of spermatogenesis and is maintained during adulthood. Importantly, this is the time at which we observed the establishment of the phenotype in the testis of the mutant animals.

RanBPM functions in a cell-autonomous way in the male germ cells

Because *RanBPM* is expressed in both germ cells and supporting cells, we investigated next whether the spermatogenesis defect observed in the mutant mice was caused by a defect in the Sertoli

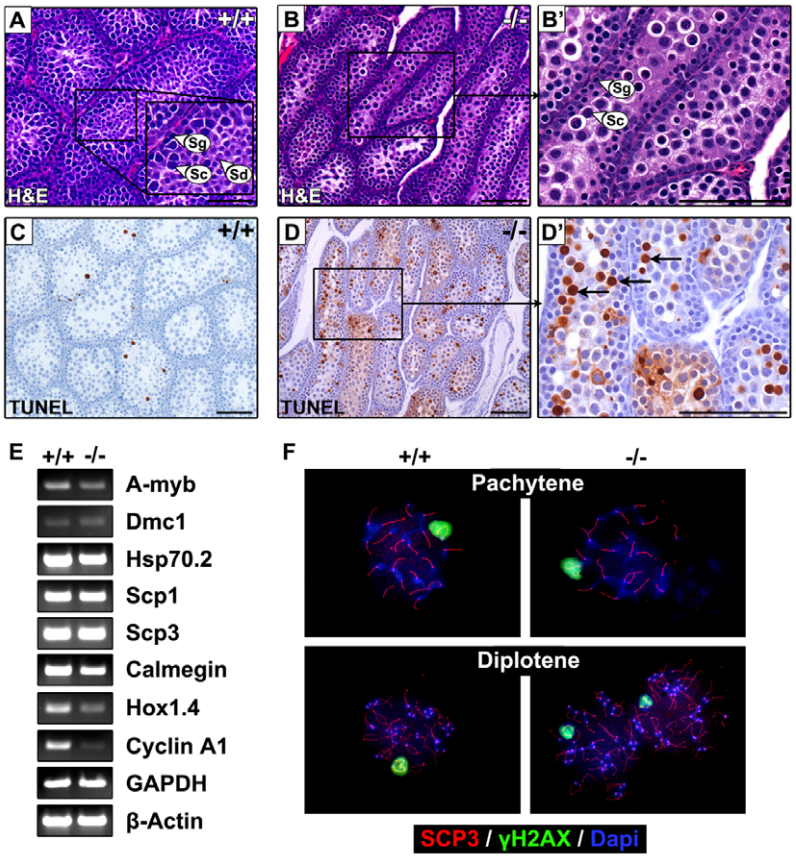

Fig. 4. Disruption of the first wave of spermatogenesis in *RanBPM*$^{-/-}$ mice. (**A-D**) Wild-type (WT; A,C) and *RanBPM*$^{-/-}$ (B,D) 3-week-old testis sections stained with Hematoxylin and Eosin (H&E; A,B) or processed for TUNEL assay (C,D) show a lack of spermatids and a high level of germ cell apoptosis (brown cells indicated by black arrows) in the mutant (compare C and D). B′ and D′ are high magnification images of boxed areas in B and D, respectively. Sg, spermatogonia; Sc, spermatocyte; Sd, spermatid. Scale bars: 100 μm. (**E**) RT-PCR analysis for stage-specific markers of spermatogenesis on 3-week-old WT and knockout testes. GAPDH and β-Actin were used as standards. (**F**) Analysis of meiotic progression of spermatocytes. Immunofluorescence labeling of spermatocyte spreads at pachytene (top panels) and diplotene (bottom panels) from 3-week-old WT and *RanBPM*$^{-/-}$ mice. The synaptonemal complex (SC) was labeled with anti-Scp3 antibodies (red). The sex body was visualized using anti-γH2AX antibodies (green) and DNA using DAPI (blue).

cell nursing function or by a cell-autonomous defect in germ cells. To this end, we inactivated the second *RanBPM* allele in the targeted ES cells used to generate the mutant mouse and injected the *RanBPM*$^{-/-}$ ES cells into recipient WT blastocysts. Blastocyst injection of heterozygous (HET) ES cells used as a control showed that these cells could give rise to both Sertoli and germ cells (Fig. 6). Seminiferous tubules from 3-week-old chimeras generated with HET ES cells were similar to those from *RanBPM*$^{+/-}$ animals and contained β-gal-positive germ cells, including spermatogonia and spermatocytes (Fig. 6C and 6A, respectively). By contrast, in chimeras generated with *RanBPM*$^{-/-}$ ES cells, seminiferous tubules contained only β-gal-negative WT germ cells, whereas Sertoli cells and most interstitial cells were β-gal-positive (Fig. 6E). Importantly, in 10-day-old chimeras, we did find tubules almost uniformly stained for β-gal, suggesting that mutant cells have the ability to produce gonocytes (Fig. 6G,H). However, these cells disappeared by 3 weeks. In chimeras generated using –/– ES cells, spermatogenesis occurred normally, as spermatids could be produced from WT cells originating from the recipient blastocyts (Fig. 6F). As the supporting cells in these chimeras were derived from –/– ES cells, we suggest that *RanBPM* expression in Sertoli and interstitial cells is not required to support spermatogenesis (compare Fig. 6B,D and F). By contrast, the complete absence of germ cells coming from mutant ES cells in pubertal animals suggests that RanBPM acts in a cell-autonomous way in gonocytes and is crucial for the germ cell lineage.

RanBPM$^{-/-}$ females display a premature ovarian failure

Mating for a two-month period of 7- to 8-week-old *RanBPM*$^{-/-}$ females (n=6) to WT males failed to produce any offspring despite the presence of plugs. This observation suggested that mutant females are sterile similarly to *RanBPM*$^{-/-}$ males. Indeed, they displayed ovaries greatly reduced in size and containing only few follicles (Fig. 7). A significant decrease in the number of primary follicles was already apparent at 3 weeks of age (Fig. 7A,B) and very few follicles were detected at 2 months (Fig. 7C,D). By 7 months, mutant ovaries were cystic and devoid of follicles (Fig. 7E,F). As premature ovarian failure can result from a number of defects affecting, for example, PGC migration, the meiotic process, and the formation, survival, activation and development of primordial follicles (for a review, see Jagarlamudi et al., 2010), we first analyzed mutant ovaries starting at E17.5. At this stage, γH2AX staining did not show any abnormality in the number of meiotic oocytes, suggesting that PGC migration occurred normally (Fig. 8A,B). However, at birth, when oocytes are reaching the end of prophase I, double labeling for MVH and γH2AX showed an already sharp decrease in the number of oocytes in *RanBPM*$^{-/-}$ ovaries (Fig. 8C,D). Moreover, the percentage of TUNEL-labeled oocytes in P0 mutant ovaries was significantly higher (~20% of the total oocytes) than that detected in WT (~5% of the total oocytes; data not shown), suggesting that oocytes are lost by apoptosis between E17.5 and P0. Analysis of oocytes at P2 and P5 using the MVH marker confirmed that most oocytes were already lost before those stages (Fig. 8E,F; data not shown). The loss of oocytes at birth suggests an arrest of oocyte differentiation at the end of prophase I. *RanBPM* expression, analyzed by β-Gal staining in heterozygous females, showed that at E17.5 this gene is not present in ovaries (data not shown). Its expression was detected at birth when the oocytes are reaching the dictyate arrest at the end of prophase I (Fig. 8G,H). Most importantly, the onset of *RanBPM* expression in oocytes coincides with the time at which oocytes are lost in the mutant animals, suggesting a crucial and germ cell-

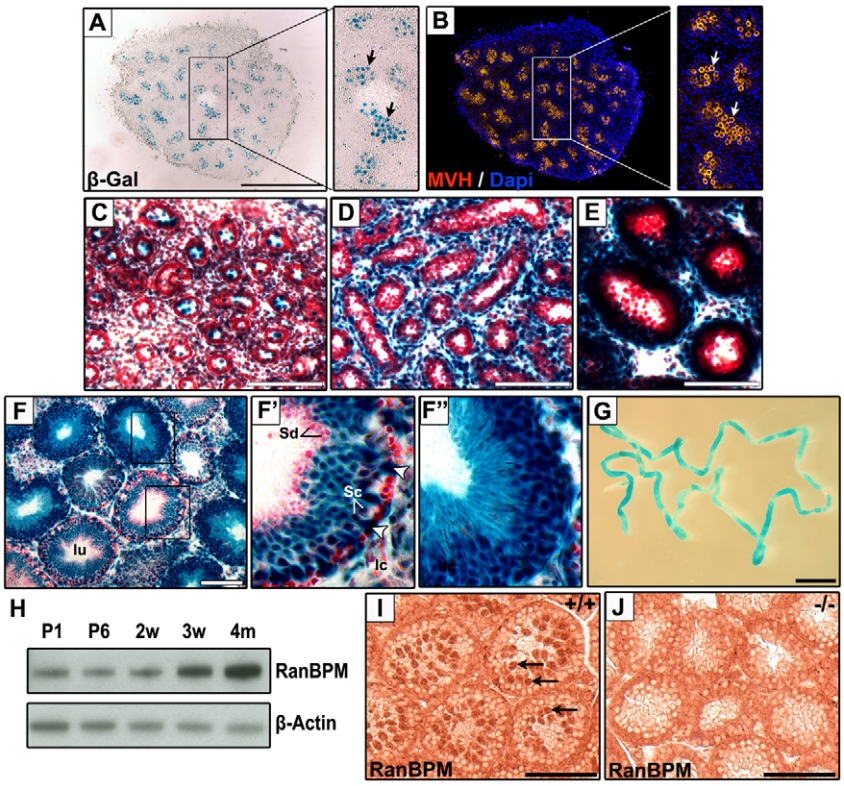

Fig. 5. Developmental expression of RanBPM in testis. (**A**,**B**) β-Galactosidase (β-gal) staining of heterozygous mice testes showing *RanBPM* expression at embryonic stage (E)17.5 (A) and its colocalization with the germ cell marker MVH (B). (**C-E**) β-Gal staining of *RanBPM*$^{+/-}$ testes at birth (C), postnatal day (P)5 (D) and 2 weeks (E). Staining duration was identical for sections C to E. Counterstaining was performed using Neutral Red. (**F-G**) β-Gal staining of adult *RanBPM*$^{+/-}$ testis sections (F) and whole-mount seminiferous tubules (G), showing a high and dynamic expression of *RanBPM* at different stages of the seminiferous tubule cycle. F′ and F″ are high magnification images of insets in F showing a high level of expression in the germinal cell lineage. Note the high level of expression in spermatocytes (Sc in F′) and Sertoli cells (white arrowheads). lu, lumen; lc, Leydig cells; Sd, spermatids. Scale bars: 400 μm in A; 100 μm in C-F; 2 mm in G. (**H-J**) RanBPM protein is expressed and upregulated during testis maturation. (H) Western blot analysis of whole testis lysates from P1 to 4 months using an anti-RanBPM antibody. β-Actin was used as loading control. (I-J) RanBPM protein is detected by immunohistochemistry in spermatocytes from 2.5-week-old wild-type (WT; I) testis sections but not in age-matched mutant sections (J). Scale bar: 100 μm.

autonomous role for RanBPM in the ovary. In addition, pubertal females displayed cyclic changes in vaginal impedance indicative of normal estrus cycles (data not shown), which suggests that follicle and stromal cell functions are not affected and that RanBPM plays an oocyte-intrinsic role.

Although *RanBPM* expression was observed in some somatic cells, such as the endocrine theca cells of ovarian follicles developing in the adult ovary, the highest expression of *RanBPM* was detected in the oocyte (Fig. 9). Moreover, its expression was maintained in the oocyte during follicle maturation, from primary to Graafian follicles (Fig. 9B,C).

Follicles are able to mature in *RanBPM*$^{-/-}$ ovaries

Because *RanBPM* is expressed in the oocyte during adulthood and mutant ovaries still contain few oocytes, we investigated whether, in addition to being crucial for normal oocyte development,

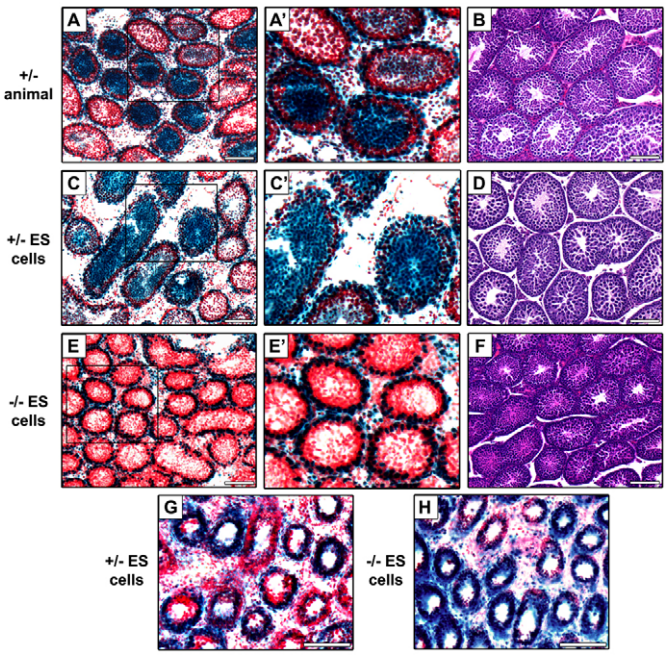

Fig. 6. Cell-autonomous role of RanBPM in germ cells. (**A**,**A′**,**C**,**C′**,**E**,**E′**) β-Galactosidase (β-gal) staining of 23-day-old (P23) testis sections from heterozygous (+/–; A,A′) animals or chimeras generated by blastocyst injection of heterozygous (+/– ES cells; C,C′) or mutant (–/– ES cells; E,E′) embryonic stem cells shows a total lack of β-gal+ germ cells in the tubules of chimeras generated with the –/– ES cells (E,E′). Note the abundant staining in the supporting cells surrounding the tubules in E and E′. (**G**,**H**) β-Gal staining of 10-day-old chimeras generated by either +/– (G) or –/– (H) ES cells showing no difference in the contribution of the ES cells to the tubules of either type of chimeras (H). (**B**,**D**,**F**) Corresponding Hematoxylin and Eosin (H&E) staining of P23 testis sections from heterozygous animal (B) or chimeras generated from +/– (D) or –/– (F) ES cell injection. Scale bars: 100 μm.

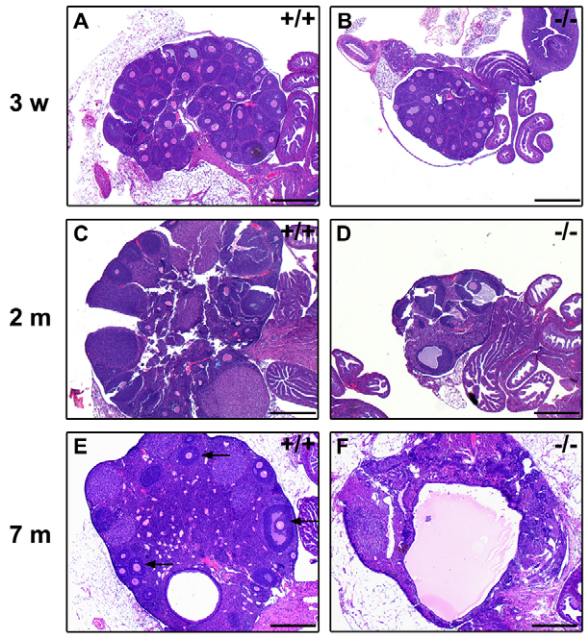

Fig. 7. Atrophy of *RanBPM*$^{-/-}$ ovaries. (**A-F**) Histological analysis of ovary Hematoxylin and Eosin (H&E) sections of wild-type (WT; A,C,E) and mutant (B,D,F) mice at 3 weeks (A,B), 2 months (C,D) and 7 months (E,F). At 3 weeks, ovaries are already atrophied and contain fewer follicles than WT. At 2 months, only a few follicles are present in *RanBPM*$^{-/-}$ mice ovaries and by 7 months mutant ovaries are devoid of follicles. Note that the apparent similar size between aged mutant (F) and control (E) ovaries is due to the presence of a large cyst in the mutant. Arrows in E indicate follicles. Scale bars: 500 μm.

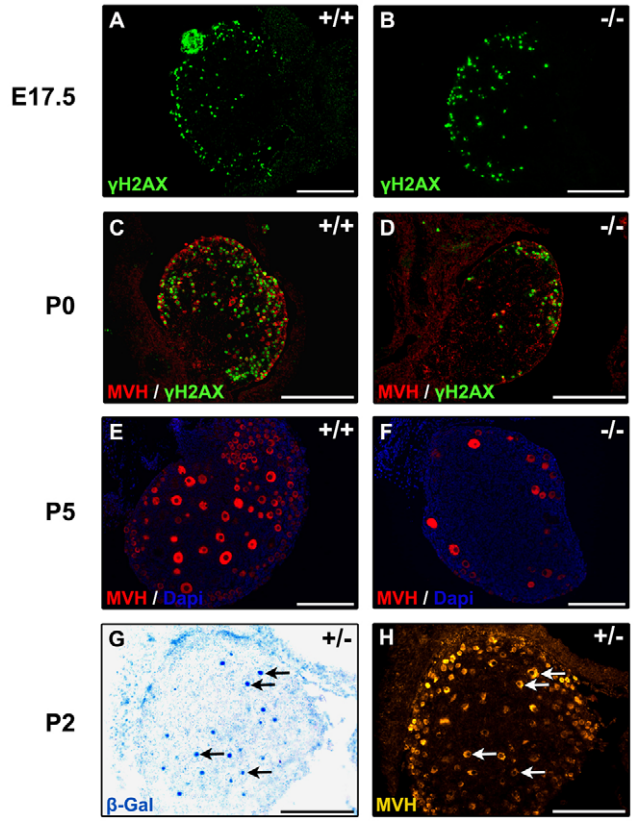

Fig. 8. Perinatal loss of oocytes in *RanBPM*$^{-/-}$ mice. (**A**,**B**) γH2AX-immunostained ovary cryosections showing comparable numbers of meiotic oocytes between wild-type (WT; A) and *RanBPM*$^{-/-}$ (B) embryonic day (E)17.5 animals. (**C**,**D**) Immunolabeling of germ cells using anti-MVH (red) and anti-γH2AX (green) antibodies on paraffin ovary sections from postnatal day (P)0 WT (C) and *RanBPM*$^{-/-}$ (D) mice. Note the oocyte depletion at this stage in the mutant ovaries. (**E**,**F**) Immunolabeling for MVH on paraffin ovary sections from P5 WT (E) and *RanBPM*$^{-/-}$ (F) mice. Sections counterstained with DAPI (blue). (**G**,**H**) β-Gal staining of a P2 heterozygous ovary section showing a population of *RanBPM*-expressing oocytes (blue) (G). Immunolabeling of germ cells using anti-MVH antibodies on the same section (H). Arrows indicate a sample of oocytes co-expressing *RanBPM* and MVH. Scale bars: 200 μm.

RanBPM could also have a role in the maturation of ovarian follicles (Eppig et al., 2002). Analysis of ovaries from superovulated 3-week-old mice showed that mutant ovaries can form follicles to the antral stage (Fig. 9D,E). The few oocytes still present appeared normal and, relative to the ovary size, the level of apoptosis was comparable to control animals (Fig. 9F,G). Taken together, these data suggest that RanBPM does not play an essential role in the control of follicle maturation in the adult ovary, but rather affects oocyte development per se.

DISCUSSION

RanBPM is a scaffolding protein that has been involved in a variety of biological processes, particularly in the immune and nervous system (Murrin and Talbot, 2007). However, as RanBPM interacts with a broad spectrum of proteins, including membrane receptors and cytoplasmic and nuclear proteins that are functionally unrelated, its physiological role is still unknown. Here, we show that RanBPM is not essential for mouse embryonic development. However, both mouse genders are sterile because of a potentially related germ cell defect.

RanBPM expression in reproductive organs starts only in late embryonic development, both in males and females, and, at that time, is restricted to germ cells. In agreement with this expression profile, *RanBPM* deletion does not affect PGC migration, as gonocytes were present in seminiferous tubules at birth and E17.5 ovaries contained normal numbers of oocytes. Interestingly, in both males and females, defects were noted at the time at which germ cells enter meiosis.

The prophase of the first meiotic division involves genetic recombination, pairing of homologous chromosomes and formation of the synaptonemal complex (SC). SCs are zipper-like structures that are assembled between the chromosomes pairs at the pachytene stage (Cohen and Pollard, 2001; Zickler and Kleckner, 1999). The disruption of various genes leads to meiotic arrest and subsequent apoptotic cell death in the testis (Cooke and Saunders, 2002; de Rooij and de Boer, 2003; Matzuk and Lamb, 2002). For example, in mice with null mutations in the DNA repair gene *Msh4* (Kneitz et al., 2000), the cyclin-dependent kinase 2 *Cdk2* (Berthet et al., 2003; Ortega et al., 2003; Viera et al., 2009), the RecA-like gene *Dmc1* (Yoshida et al., 1998), the ataxia-telangiectasia mutated gene *Atm* (Xu et al., 1996) or the synaptonemal complex protein *Scp3* (Yuan et al., 2000), chromosomes fail to undergo normal pairing causing cell death during prophase I. Moreover, recent studies indicated the existence of a pachytene checkpoint that prevents nuclear division when there is a failure in recombination

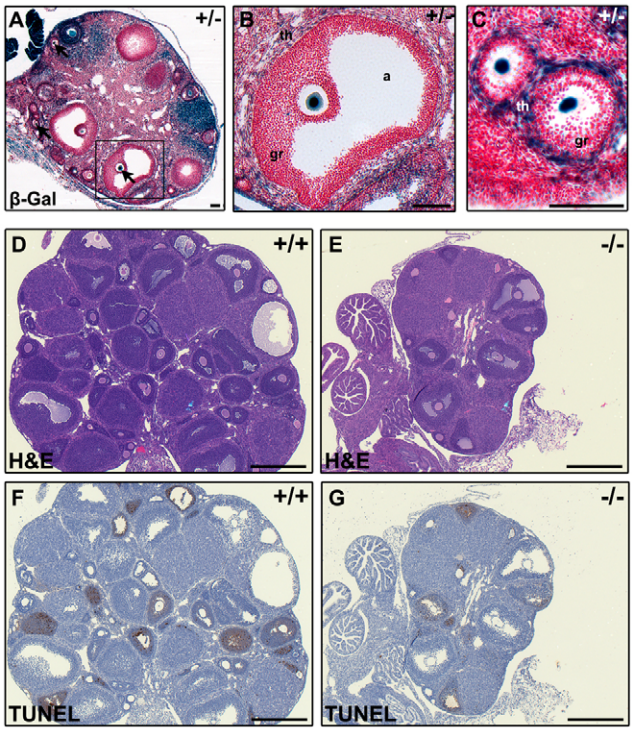

Fig. 9. RanBPM is not required for follicle maturation in the adult mouse ovary. (**A-C**) β-Gal staining of adult *RanBPM* heterozygous ovary sections showing prominent labeling of the oocyte in follicles at different stages of maturation (arrows in A). B displays a higher magnification picture of the Graafian follicle shown in A. C shows *RanBPM* expression in primary follicles. *RanBPM* is also expressed in the flattened thecal cells (th) of the follicles. Sections counterstained with Neutral Red. gr, granulosa; a, antrum. Scale bars: 100 μm. (**D-G**) Hematoxylin and Eosin (H&E; D,E) and TUNEL (F,G) staining of ovary sections from 3-week-old superovulated wild-type (WT; D,F) and *RanBPM*$^{-/-}$ (E,G) females showing the presence of secondary (antral) follicles in the *RanBPM*$^{-/-}$ ovary and no significant difference in apoptosis between control and mutant superovulated ovaries. Scale bars: 500 μm.

or synapsis (Roeder and Bailis, 2000). In 3-week-old *RanBPM*$^{-/-}$ males, the expression levels of pachytene stage-specific genes such as *Scp1* and *Scp3* (Klink et al., 1997; Meuwissen et al., 1992) were normal. In addition, analysis of the structure of SCs showed that chromosome synapsis occurred normally in mutant pachytene spermatocytes. However, taking into account the upregulation of *RanBPM* in spermatocytes, the predominant expression of the protein in this cell type, and the apoptotic elimination of these cells during the first wave of spermatogenesis, we cannot exclude a role for RanBPM in the meiotic process.

Adult mutant females exhibited ovaries showing dysgenesis from an absence of oocytes. Premature ovarian failure has numerous causes (for reviews, see Jagarlamudi et al., 2010; Skillern and Rajkovic, 2008). The premature ovarian failure observed in *RanBPM*$^{-/-}$ mice was directly linked to an early depletion of the oocyte pool. Interestingly, *RanBPM* expression in the ovary starts only at birth in oocytes that are probably at the late pachytene or diplotene stage. Mutant oocytes thus seem to reach the pachytene stage normally, but, as in males, germ cell differentiation is arrested at the end of prophase I, right before oocytes reach the dictyate stage. An arrest at prophase I has been reported in female mice null for genes involved in chromosome synapsis, as in *Msh4*- or *Cdk2*-null mice (Kneitz et al., 2000; Ortega et al., 2003). However, deletion of *RanBPM* did not cause a phenotype as strong as the one observed in *Msh4*- or *Cdk2*-null mice, as some follicles are still present in postnatal *RanBPM*$^{-/-}$ ovaries. In mutants for the transcription factor FIGα (Figla – Mouse Genome Informatics), in which the process of primordial follicle formation is affected, oocyte numbers are normal at birth and germ cells are lost between P0 and P1 (Soyal et al., 2000). By comparison, the phenotype of *RanBPM*$^{-/-}$ females is more close to the phenotype of mutants for genes involved in the prophase of the first meiotic division, for example *Dmc1*, in which oocytes are lost between E17.5 and P0 (Yoshida et al., 1998). Moreover, this period corresponds to the late pachytene-diplotene, which is the time at which defects are observed in males. An arrest at the same stage of meiosis in both genders suggests the presence of a common mechanism between males and females occurring at the end of prophase I. Interestingly, mutations in several genes that are involved in the mechanisms of chromosome synapsis and recombination display sex-specific effects (Hunt and Hassold, 2002). The presence of remaining oocytes could also be explained by the fact that, even if RanBPM had a role in chromosome synapsis, this could be through its scaffolding functions, by interacting with some proteins that are directly involved in this crucial process. The ability to induce maturation of the few residual oocytes in females by superovulation supports the notion that RanBPM is required at an early stage of germ cell differentiation and not at later stages such as the orchestration of follicle maturation.

In *RanBPM*$^{-/-}$ testes, spermatocytes at the late pachytene-diplotene stage were eliminated by apoptosis and, shortly after that, all germ cells disappeared leading to Sertoli-cell-only seminiferous tubules followed by tubular degeneration. Therefore, in the developing *RanBPM*$^{-/-}$ testes, only a single and abnormal postnatal wave of spermatogenesis takes place, followed by a failure of germ cells to differentiate further. Indeed, transit-amplifying spermatogonia, labeled by BrdU incorporation, were already missing at 1 month of age (data not shown) suggesting a lack of spermatogonial stem cell (SSC) renewal. Thus, in addition to the meiotic arrest occurring during the first round of spermatogenesis, spermatogonia, which are essential to continuously provide differentiating cells and maintain the spermatogenesis process, might also be affected in their survival, differentiation or self-renewal processes by the lack of RanBPM (Oatley and Brinster, 2008).

A few genes that are important for the spermatogenesis process have been reported to interact with RanBPM, suggesting a possible functional interaction. For example, the mouse vasa homolog gene (*Mvh*; *Ddx4* – Mouse Genome Informatics), encoding an ATP-dependent RNA helicase, is crucial for the development of male germ cells (Shibata et al., 2004; Tanaka et al., 2000). However, in *Mvh*-null males, germ cell differentiation stops earlier than in *RanBPM*$^{-/-}$ mice, at the zygotene stage of prophase I, and *Mvh*$^{-/-}$ females are fertile. The androgen receptor (AR) has also been reported to interact with RanBPM (Rao et al., 2002). Yet, AR knockout in the testis generates a phenotype clearly worse than the one observed in *RanBPM*$^{-/-}$ males as it leads to an abdominal localization of the testes and the absence of epididymis (Wang et al., 2009). Moreover, in contrast with *RanBPM*$^{-/-}$ females, AR-mutant females are subfertile, showing a gradual decrease in the number of follicles starting only at 3 weeks of postnatal life and probably caused by a defect in the maintenance of folliculogenesis

(Shiina et al., 2006). The fact that none of these mutants has a phenotype similar to the one caused by the RanBPM deletion reinforces the hypothesis that this gene might function as a scaffolding protein involved in multiple pathways.

Up to one week after birth, *RanBPM*$^{-/-}$ testes developed normally. However, starting at postnatal day 8 we observed a significant decrease in spermatogonia proliferation without a change in the level of apoptosis, suggesting a lack of proliferation as the main cause of the testis growth defect. To date, only a few molecules have been shown to affect germ cell proliferation in the testis, the main one being the tyrosine kinase receptor Kit, which is also implicated in germ cell survival (Blume-Jensen et al., 2000; Kissel et al., 2000). RanBPM has been shown to interact with other tyrosine kinase receptors such as Met, TrkA (Ntrk1 – Mouse Genome Informatics) and TrkB (Ntrk2 – Mouse Genome Informatics) (Wang et al., 2002; Yin et al., 2010; Yuan et al., 2006). So, it would be of interest to investigate whether RanBPM does interact with Kit also and, if so, how it would affect its signaling property. Interestingly, chimera experiments performed using *RanBPM*-null ES cells are in agreement with this hypothesis, as they suggest a cell-autonomous role for RanBPM in germ cells, the same cell population that express Kit. Importantly, as RanBPM has been described as a scaffolding protein, a phenotype involving Kit would not be incompatible with other roles of RanBPM, such as in meiosis.

Intriguingly, a null RanBPM *Drosophila* mutant in genetic mosaics indicates that RanBPM regulates the cell shape, size and organization of the germinal stem cell (GSC) niche, implicating RanBPM in the control of niche capacity for GSCs (Dansereau and Lasko, 2008). Although *Drosophila* and mammals are evolutionarily distant, it is interesting to observe that the *RanBPM* gene has a conserved role in reproduction in both species. In the future, it will be of interest to identify the signaling pathways affected in *RanBPM*$^{-/-}$ mice and to investigate whether, in addition to its role in reproductive organs, the functional similarities between species extend even to the molecular level.

In summary, RanBPM affects gametogenesis in both genders, suggesting that this scaffolding protein modulates the function of multiple genes involved in the meiosis process and/or affects growth factor signaling pathways controlling germ cell proliferation, survival and renewal.

Acknowledgements

We would like to thank Drs Shyam Sharan and Esta Sterneck for helpful discussions; Susan Reid, Eileen Southon and Donna Butcher for excellent technical assistance; and Dr A. F. Parlow for performing the hormone measurements. This research was supported by the Intramural Research Program of the NCI, Center for Cancer Research, NIH. Deposited in PMC for release after 12 months.

Competing interests statement

The authors declare no competing financial interests.

References

Beddow, A. L., Richards, S. A., Orem, N. R. and Macara, I. G. (1995). The Ran/TC4 GTPase-binding domain: identification by expression cloning and characterization of a conserved sequence motif. *Proc. Natl. Acad. Sci. USA* **92**, 3328-3332.

Berthet, C., Aleem, E., Coppola, V., Tessarollo, L. and Kaldis, P. (2003). Cdk2 knockout mice are viable. *Curr. Biol.* **13**, 1775-1785.

Blume-Jensen, P., Jiang, G., Hyman, R., Lee, K. F., O'Gorman, S. and Hunter, T. (2000). Kit/stem cell factor receptor-induced activation of phosphatidylinositol 3′-kinase is essential for male fertility. *Nat. Genet.* **24**, 157-162.

Chang, Y., Paramasivam, M., Girgenti, M. J., Walikonis, R. S., Bianchi, E. and LoTurco, J. J. (2010). RanBPM regulates the progression of neuronal precursors through M-phase at the surface of the neocortical ventricular zone. *Dev. Neurobiol.* **70**, 1-15.

Cheng, L., Lemmon, S. and Lemmon, V. (2005). RanBPM is an L1-interacting protein that regulates L1-mediated mitogen-activated protein kinase activation. *J. Neurochem.* **94**, 1102-1110.

Cohen, P. E. and Pollard, J. W. (2001). Regulation of meiotic recombination and prophase I progression in mammals. *BioEssays* **23**, 996-1009.

Cooke, H. J. and Saunders, P. T. (2002). Mouse models of male infertility. *Nat. Rev. Genet.* **3**, 790-801.

Dansereau, D. A. and Lasko, P. (2008). RanBPM regulates cell shape, arrangement, and capacity of the female germline stem cell niche in Drosophila melanogaster. *J. Cell Biol.* **182**, 963-977.

de Rooij, D. G. and de Boer, P. (2003). Specific arrests of spermatogenesis in genetically modified and mutant mice. *Cytogenet. Genome Res.* **103**, 267-276.

Denti, S., Sirri, A., Cheli, A., Rogge, L., Innamorati, G., Putignano, S., Fabbri, M., Pardi, R. and Bianchi, E. (2004). RanBPM is a phosphoprotein that associates with the plasma membrane and interacts with the integrin LFA-1. *J. Biol. Chem.* **279**, 13027-13034.

Emes, R. D. and Ponting, C. P. (2001). A new sequence motif linking lissencephaly, Treacher Collins and oral-facial-digital type 1 syndromes, microtubule dynamics and cell migration. *Hum. Mol. Genet.* **10**, 2813-2820.

Eppig, J. J., Wigglesworth, K. and Pendola, F. L. (2002). The mammalian oocyte orchestrates the rate of ovarian follicular development. *Proc. Natl. Acad. Sci. USA* **99**, 2890-2894.

Gerlitz, G., Darhin, E., Giorgio, G., Franco, B. and Reiner, O. (2005). Novel functional features of the Lis-H domain: role in protein dimerization, half-life and cellular localization. *Cell Cycle* **4**, 1632-1640.

Hunt, P. A. and Hassold, T. J. (2002). Sex matters in meiosis. *Science* **296**, 2181-2183.

Jagarlamudi, K., Reddy, P., Adhikari, D. and Liu, K. (2010). Genetically modified mouse models for premature ovarian failure (POF). *Mol. Cell. Endocrinol.* **315**, 1-10.

Kim, M. H., Cooper, D. R., Oleksy, A., Devedjiev, Y., Derewenda, U., Reiner, O., Otlewski, J. and Derewenda, Z. S. (2004). The structure of the N-terminal domain of the product of the lissencephaly gene Lis1 and its functional implications. *Structure* **12**, 987-998.

Kissel, H., Timokhina, I., Hardy, M. P., Rothschild, G., Tajima, Y., Soares, V., Angeles, M., Whitlow, S. R., Manova, K. and Besmer, P. (2000). Point mutation in kit receptor tyrosine kinase reveals essential roles for kit signaling in spermatogenesis and oogenesis without affecting other kit responses. *EMBO J.* **19**, 1312-1326.

Klink, A., Lee, M. and Cooke, H. J. (1997). The mouse synaptosomal complex protein gene Sycp3 maps to band C of chromosome 10. *Mamm. Genome* **8**, 376-377.

Kneitz, B., Cohen, P. E., Avdievich, E., Zhu, L., Kane, M. F., Hou, H., Jr, Kolodner, R. D., Kucherlapati, R., Pollard, J. W. and Edelmann, W. (2000). MutS homolog 4 localization to meiotic chromosomes is required for chromosome pairing during meiosis in male and female mice. *Genes Dev.* **14**, 1085-1097.

Kobayashi, N., Yang, J., Ueda, A., Suzuki, T., Tomaru, K., Takeno, M., Okuda, K. and Ishigatsubo, Y. (2007). RanBPM, Muskelin, p48EMLP, p44CTLH, and the armadillo-repeat proteins ARMC8alpha and ARMC8beta are components of the CTLH complex. *Gene* **396**, 236-247.

Lakshmana, M. K., Yoon, I. S., Chen, E., Bianchi, E., Koo, E. H. and Kang, D. E. (2009). Novel role of RanBP9 in BACE1 processing of amyloid precursor protein and amyloid beta peptide generation. *J. Biol. Chem.* **284**, 11863-11872.

Mahadevaiah, S. K., Turner, J. M., Baudat, F., Rogakou, E. P., de Boer, P., Blanco-Rodriguez, J., Jasin, M., Keeney, S., Bonner, W. M. and Burgoyne, P. S. (2001). Recombinational DNA double-strand breaks in mice precede synapsis. *Nat. Genet.* **27**, 271-276.

Matzuk, M. M. and Lamb, D. J. (2002). Genetic dissection of mammalian fertility pathways. *Nat. Cell Biol.* **4 Suppl.**, S41-S49.

Menon, R. P., Gibson, T. J. and Pastore, A. (2004). The C terminus of fragile X mental retardation protein interacts with the multi-domain Ran-binding protein in the microtubule-organising centre. *J. Mol. Biol.* **343**, 43-53.

Mettus, R. V., Litvin, J., Wali, A., Toscani, A., Latham, K., Hatton, K. and Reddy, E. P. (1994). Murine A-myb: evidence for differential splicing and tissue-specific expression. *Oncogene* **9**, 3077-3086.

Meuwissen, R. L., Offenberg, H. H., Dietrich, A. J., Riesewijk, A., van Iersel, M. and Heyting, C. (1992). A coiled-coil related protein specific for synapsed regions of meiotic prophase chromosomes. *EMBO J.* **11**, 5091-5100.

Murrin, L. C. and Talbot, J. N. (2007). RanBPM, a scaffolding protein in the immune and nervous systems. *J. Neuroimmune Pharmacol.* **2**, 290-295.

Nishitani, H., Hirose, E., Uchimura, Y., Nakamura, M., Umeda, M., Nishii, K., Mori, N. and Nishimoto, T. (2001). Full-sized RanBPM cDNA encodes a protein possessing a long stretch of proline and glutamine within the N-terminal region, comprising a large protein complex. *Gene* **272**, 25-33.

Oatley, J. M. and Brinster, R. L. (2008). Regulation of spermatogonial stem cell self-renewal in mammals. *Annu. Rev. Cell Dev. Biol.* **24**, 263-286.

Ortega, S., Prieto, I., Odajima, J., Martin, A., Dubus, P., Sotillo, R., Barbero, J. L., Malumbres, M. and Barbacid, M. (2003). Cyclin-dependent kinase 2 is

essential for meiosis but not for mitotic cell division in mice. *Nat. Genet.* **35**, 25-31.
Page, S. L. and Hawley, R. S. (2004). The genetics and molecular biology of the synaptonemal complex. *Annu. Rev. Cell Dev. Biol.* **20**, 525-558.
Peters, A. H., Plug, A. W., van Vugt, M. J. and de Boer, P. (1997). A drying-down technique for the spreading of mammalian meiocytes from the male and female germline. *Chromosome Res.* **5**, 66-68.
Ponting, C., Schultz, J. and Bork, P. (1997). SPRY domains in ryanodine receptors (Ca(2+)-release channels). *Trends Biochem. Sci.* **22**, 193-194.
Rao, M. A., Cheng, H., Quayle, A. N., Nishitani, H., Nelson, C. C. and Rennie, P. S. (2002). RanBPM, a nuclear protein that interacts with and regulates transcriptional activity of androgen receptor and glucocorticoid receptor. *J. Biol. Chem.* **277**, 48020-48027.
Reid, S. W. and Tessarollo, L. (2009). Isolation, microinjection and transfer of mouse blastocysts. *Methods Mol. Biol.* **530**, 269-285.
Roeder, G. S. and Bailis, J. M. (2000). The pachytene checkpoint. *Trends Genet.* **16**, 395-403.
Rosario, M. O., Perkins, S. L., O'Brien, D. A., Allen, R. L. and Eddy, E. M. (1992). Identification of the gene for the developmentally expressed 70 kDa heat-shock protein (P70) of mouse spermatogenic cells. *Dev. Biol.* **150**, 1-11.
Rossi, P., Dolci, S., Sette, C., Capolunghi, F., Pellegrini, M., Loiarro, M., Di Agostino, S., Paronetto, M. P., Grimaldi, P., Merico, D. et al. (2004). Analysis of the gene expression profile of mouse male meiotic germ cells. *Gene Expr. Patterns* **4**, 267-281.
Rubin, M. R., Toth, L. E., Patel, M. D., D'Eustachio, P. and Nguyen-Huu, M. C. (1986). A mouse homeo box gene is expressed in spermatocytes and embryos. *Science* **233**, 663-667.
Shibata, N., Tsunekawa, N., Okamoto-Ito, S., Akasu, R., Tokumasu, A. and Noce, T. (2004). Mouse RanBPM is a partner gene to a germline specific RNA helicase, mouse vasa homolog protein. *Mol. Reprod. Dev.* **67**, 1-7.
Shiina, H., Matsumoto, T., Sato, T., Igarashi, K., Miyamoto, J., Takemasa, S., Sakari, M., Takada, I., Nakamura, T., Metzger, D. et al. (2006). Premature ovarian failure in androgen receptor-deficient mice. *Proc. Natl. Acad. Sci. USA* **103**, 224-229.
Skillern, A. and Rajkovic, A. (2008). Recent developments in identifying genetic determinants of premature ovarian failure. *Sex. Dev.* **2**, 228-243.
Soyal, S. M., Amleh, A. and Dean, J. (2000). FIGalpha, a germ cell-specific transcription factor required for ovarian follicle formation. *Development* **127**, 4645-4654.
Sweeney, C., Murphy, M., Kubelka, M., Ravnik, S. E., Hawkins, C. F., Wolgemuth, D. J. and Carrington, M. (1996). A distinct cyclin A is expressed in germ cells in the mouse. *Development* **122**, 53-64.
Tanaka, S. S., Toyooka, Y., Akasu, R., Katoh-Fukui, Y., Nakahara, Y., Suzuki, R., Yokoyama, M. and Noce, T. (2000). The mouse homolog of Drosophila Vasa is required for the development of male germ cells. *Genes Dev.* **14**, 841-853.
Togashi, H., Schmidt, E. F. and Strittmatter, S. M. (2006). RanBPM contributes to Semaphorin3A signaling through plexin-A receptors. *J. Neurosci.* **26**, 4961-4969.
Valiyaveettil, M., Bentley, A. A., Gursahaney, P., Hussien, R., Chakravarti, R., Kureishy, N., Prag, S. and Adams, J. C. (2008). Novel role of the muskelin-RanBP9 complex as a nucleocytoplasmic mediator of cell morphology regulation. *J. Cell Biol.* **182**, 727-739.
Viera, A., Rufas, J. S., Martinez, I., Barbero, J. L., Ortega, S. and Suja, J. A. (2009). CDK2 is required for proper homologous pairing, recombination and sex-body formation during male mouse meiosis. *J. Cell Sci.* **122**, 2149-2159.
Wang, D., Li, Z., Messing, E. M. and Wu, G. (2002). Activation of Ras/Erk pathway by a novel MET-interacting protein RanBPM. *J. Biol. Chem.* **277**, 36216-36222.
Wang, R. S., Yeh, S., Tzeng, C. R. and Chang, C. (2009). Androgen receptor roles in spermatogenesis and fertility: lessons from testicular cell-specific androgen receptor knockout mice. *Endocr. Rev.* **30**, 119-132.
Watanabe, D., Yamada, K., Nishina, Y., Tajima, Y., Koshimizu, U., Nagata, A. and Nishimune, Y. (1994). Molecular cloning of a novel Ca(2+)-binding protein (calmegin) specifically expressed during male meiotic germ cell development. *J. Biol. Chem.* **269**, 7744-7749.
Xu, Y., Ashley, T., Brainerd, E. E., Bronson, R. T., Meyn, M. S. and Baltimore, D. (1996). Targeted disruption of ATM leads to growth retardation, chromosomal fragmentation during meiosis, immune defects, and thymic lymphoma. *Genes Dev.* **10**, 2411-2422.
Yin, Y. X., Sun, Z. P., Huang, S. H., Zhao, L., Geng, Z. and Chen, Z. Y. (2010). RanBPM contributes to TrkB signaling and regulates brain-derived neurotrophic factor-induced neuronal morphogenesis and survival. *J. Neurochem.* **114**, 110-121.
Yoshida, K., Kondoh, G., Matsuda, Y., Habu, T., Nishimune, Y. and Morita, T. (1998). The mouse RecA-like gene Dmc1 is required for homologous chromosome synapsis during meiosis. *Mol. Cell* **1**, 707-718.
Yuan, L., Liu, J. G., Zhao, J., Brundell, E., Daneholt, B. and Hoog, C. (2000). The murine SCP3 gene is required for synaptonemal complex assembly, chromosome synapsis, and male fertility. *Mol. Cell* **5**, 73-83.
Yuan, Y., Fu, C., Chen, H., Wang, X., Deng, W. and Huang, B. R. (2006). The Ran binding protein RanBPM interacts with TrkA receptor. *Neurosci. Lett.* **407**, 26-31.
Zakeri, Z. F., Wolgemuth, D. J. and Hunt, C. R. (1988). Identification and sequence analysis of a new member of the mouse HSP70 gene family and characterization of its unique cellular and developmental pattern of expression in the male germ line. *Mol. Cell. Biol.* **8**, 2925-2932.
Zickler, D. and Kleckner, N. (1999). Meiotic chromosomes: integrating structure and function. *Annu. Rev. Genet.* **33**, 603-754.